# Supplementary Materials

# Small molecule-assisted synthesis of carbon supported platinum intermetallic fuel cell catalysts

Tian-Wei Song[1], Cong Xu[1], Zhu-Tao Sheng[2], Hui-Kun Yan[1], Lei Tong[1], Jun Liu[3,4], Wei-Jie Zeng[1], Lu-Jie Zuo[1], Peng Yin[1], Ming Zuo[1], Sheng-Qi Chu[5], Ping Chen[6], Hai-Wei Liang[1]*

[1]Hefei National Research Center for Physical Sciences at the Microscale, Department of Chemistry, University of Science and Technology of China, Hefei 230026, China

[2]College of Chemistry and Materials Science, Anhui Normal University, Wuhu 241000, China

[3]Institute of Solid State Physics, Hefei Institutes of Physical Science, Chinese Academy of Sciences, Hefei 230031, China

[4]Anhui Contango New Energy Technology Co., Ltd, Hefei 230088, China

[5]Institute of High Energy Physics, Chinese Academy of Sciences, Beijing 100049, China

[6]School of Chemistry and Chemical Engineering, Anhui University, Hefei 230601, China

*email: hwliang@ustc.edu.cn

## Chemicals and materials

Vanadium trichloride ($VCl_3$, 97%) and perchloric acid ($HClO_4$, 70%) were purchased from Sigma-Aldrich. Germanium chloride ($GeCl_4$, 99.9999%) were purchased from Alfa Aesar. Dicyandiamide (DCDA, 99%) was purchased from J&K Scientific Ltd. Indium chloride ($InCl_3$, 99.9%), gallium chloride ($GaCl_3$, 99.999%), 2,3-Benzofuran (99%), glucose (98%), 2-acetylpyrrole (99%), 11-Mercaptoundecanoic acid (95%), and 2-Mercaptobenzimidazole (98%) were purchased from Shanghai Macklin Biochemical Co., Ltd., China. All other chemicals were purchased from Sinopharm Chemical Reagent Co. Ltd., China, including hexachloroplatinic hexahydrate ($H_2PtCl_6 \cdot 6H_2O$, 99%), aluminium chloride ($AlCl_3 \cdot 6H_2O$, 97%), titanium tetrachloride ($TiCl_4$, 98%), chromium chloride hexahydrate ($CrCl_3 \cdot 6H_2O$, 99%), manganous chloride tetrahydrate ($MnCl_2 \cdot 4H_2O$, 99%), ferric chloride hexahydrate ($FeCl_3$, 97%), cobalt chloride hexahydrate ($CoCl_2 \cdot 6H_2O$, 99%), nickel chloride hexahydrate ($NiCl_2 \cdot 6H_2O$, 98%), copper nitrate trihydrate ($Cu(NO_3)_2 \cdot 3H_2O$, 99%), zinc nitrate hexahydrate ($Zn(NO_3)_2 \cdot 6H_2O$, 99%), stannous chloride dihydrate ($SnCl_2 \cdot 2H_2O$, 98%), sodium acetate (99.99%), sodium glycinate (98%), 1-mercaptopropane (99.5%), sodium thioglycolate (97%), and sulfuric acid ($H_2SO_4$, 95%~98%). All the chemicals were used as received without further purification. Deionized water (18.2 MΩ/cm) used in all experiments was prepared by passing through an ultra-pure purification system.

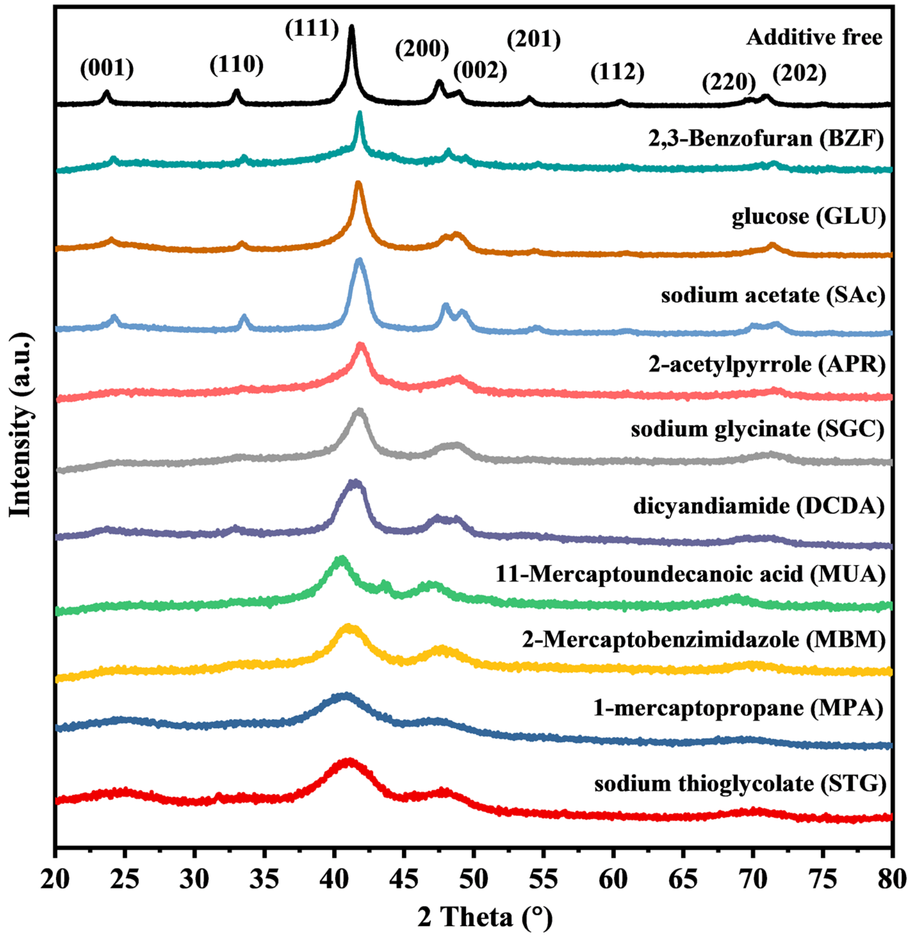


**Supplementary Figure 1.** XRD patterns of the PtCo catalysts prepared with different molecule additives. The total metal loading of all the samples were controlled to be 30 wt%.

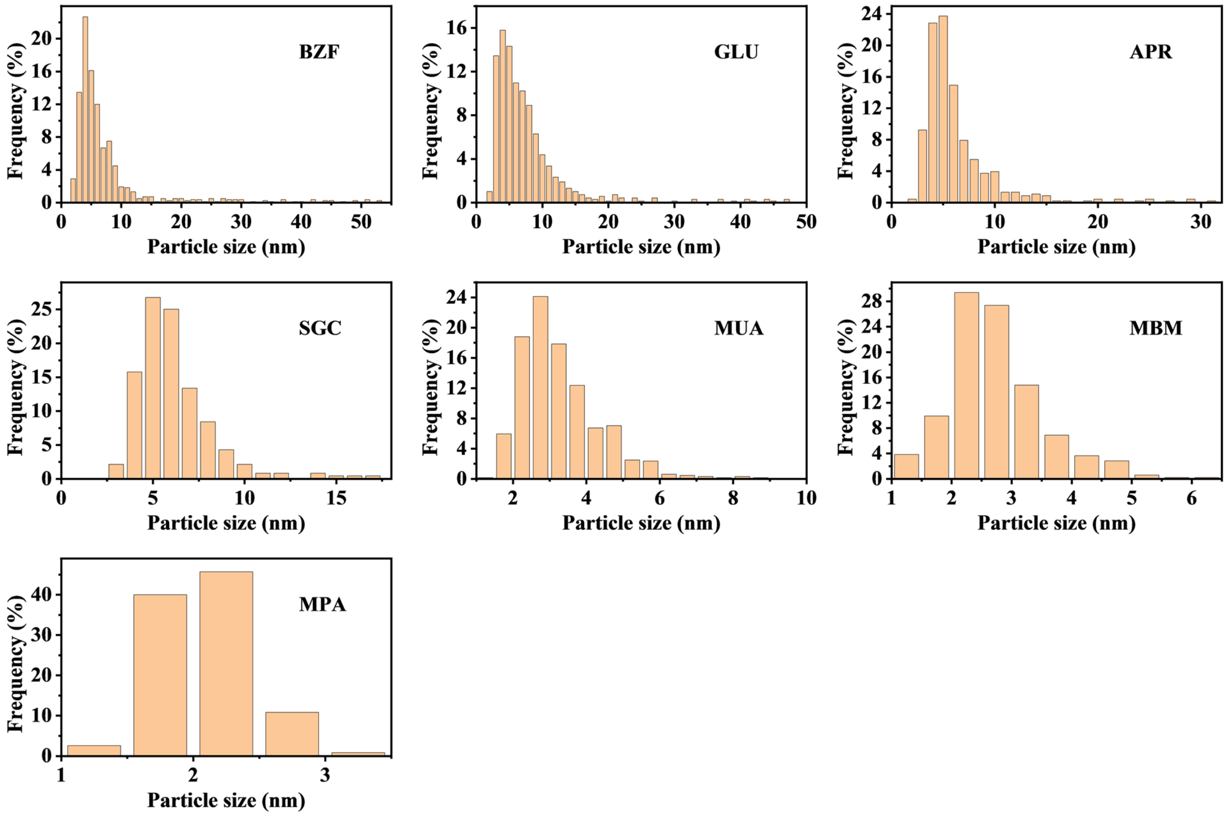


**Supplementary Figure 2.** Particle size distribution histograms of the PtCo catalysts prepared with different molecule additives, which were obtained through statistic of more than 500 particles in HAADF-STEM images.

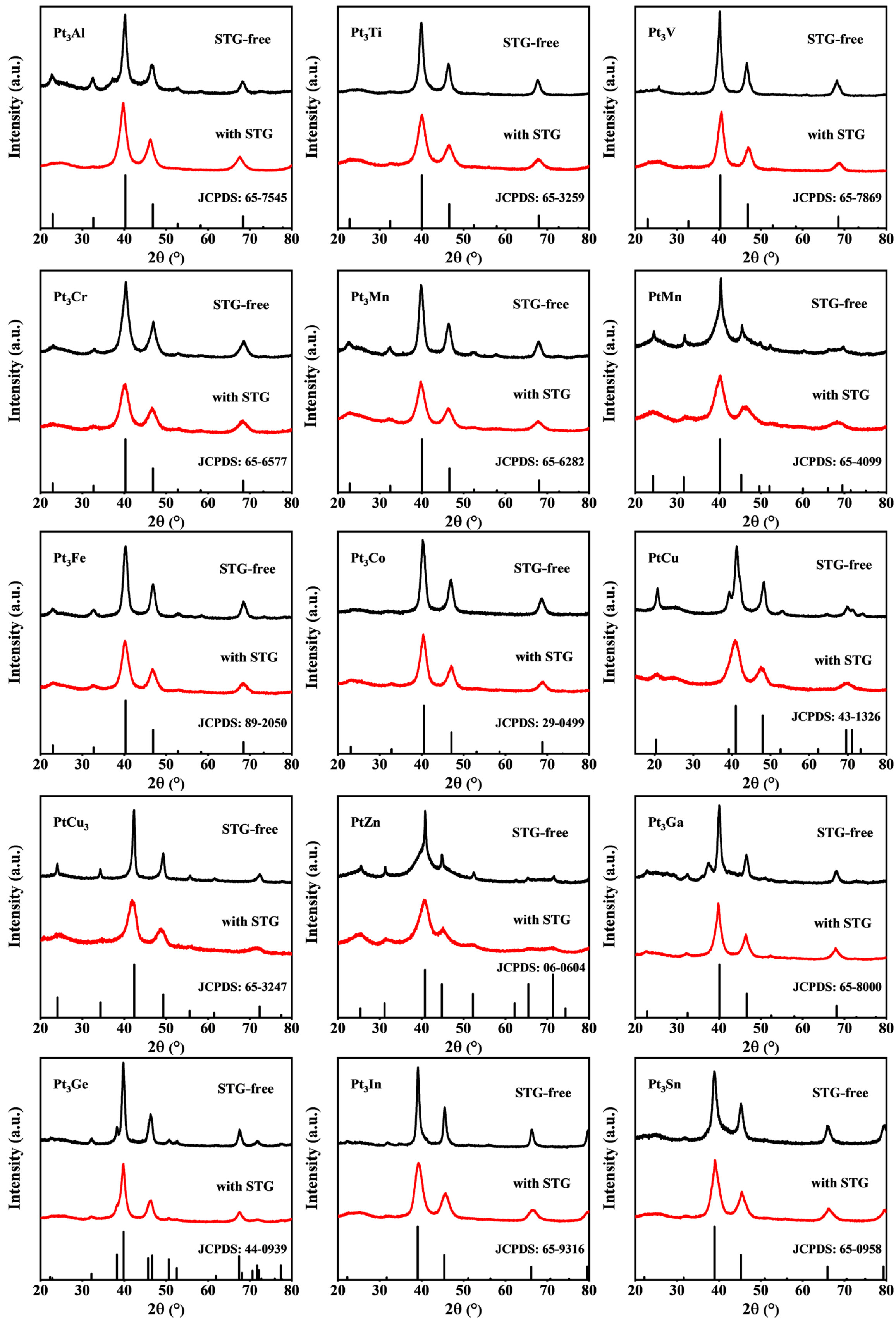


**Supplementary Figure 3.** XRD patterns of the Pt-IMCs catalysts prepared with and without STG. The JCPDS cards of the corresponding IMCs structures were also shown.

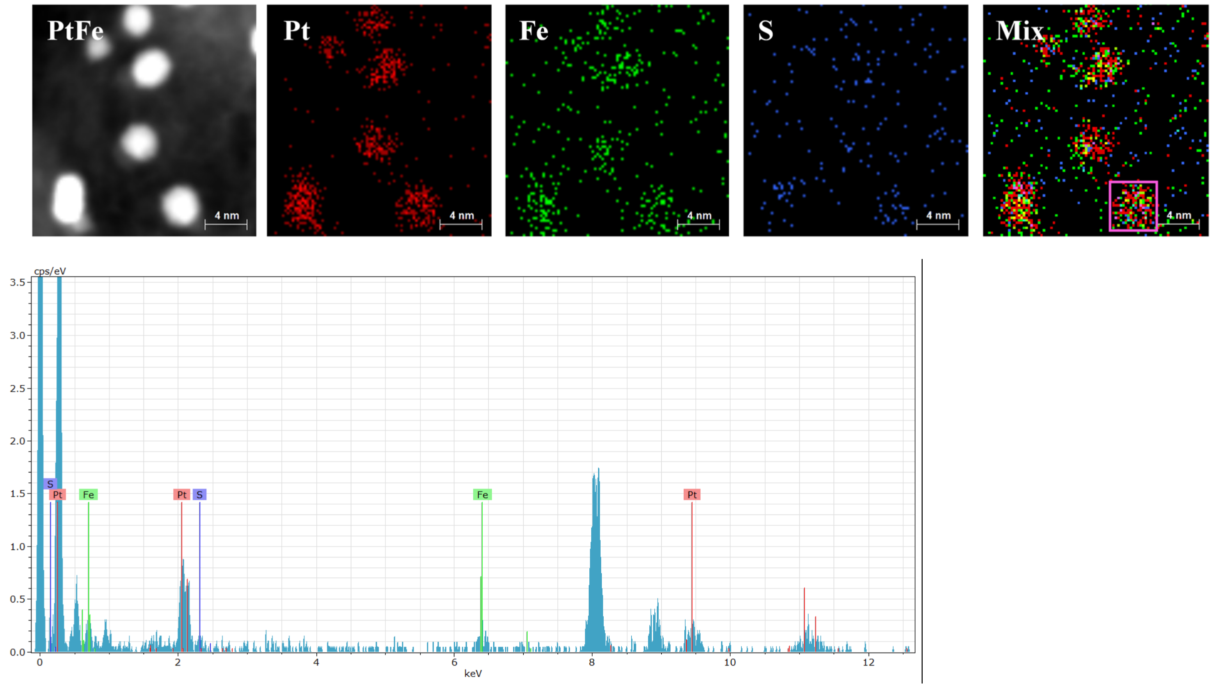


**Supplementary Figure 4.** EDS elemental mapping and EDS spectra of the PtFe IMCs catalyst.

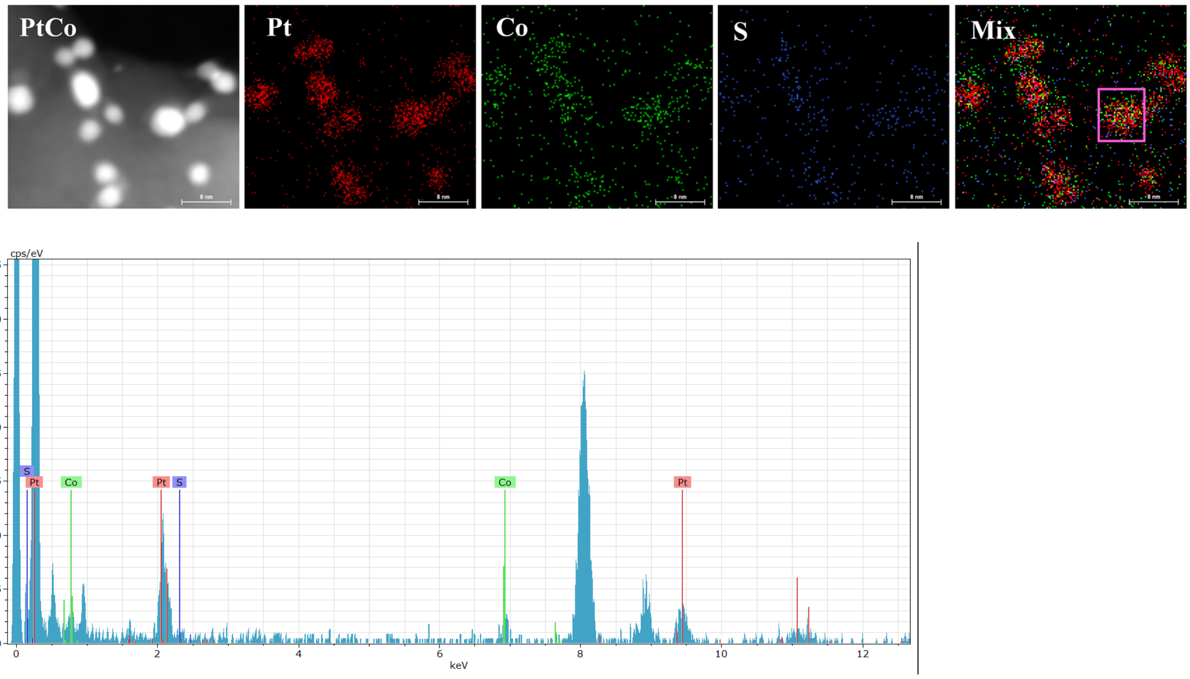


**Supplementary Figure 5.** EDS elemental mapping and EDS spectra of the PtCo IMCs catalyst.

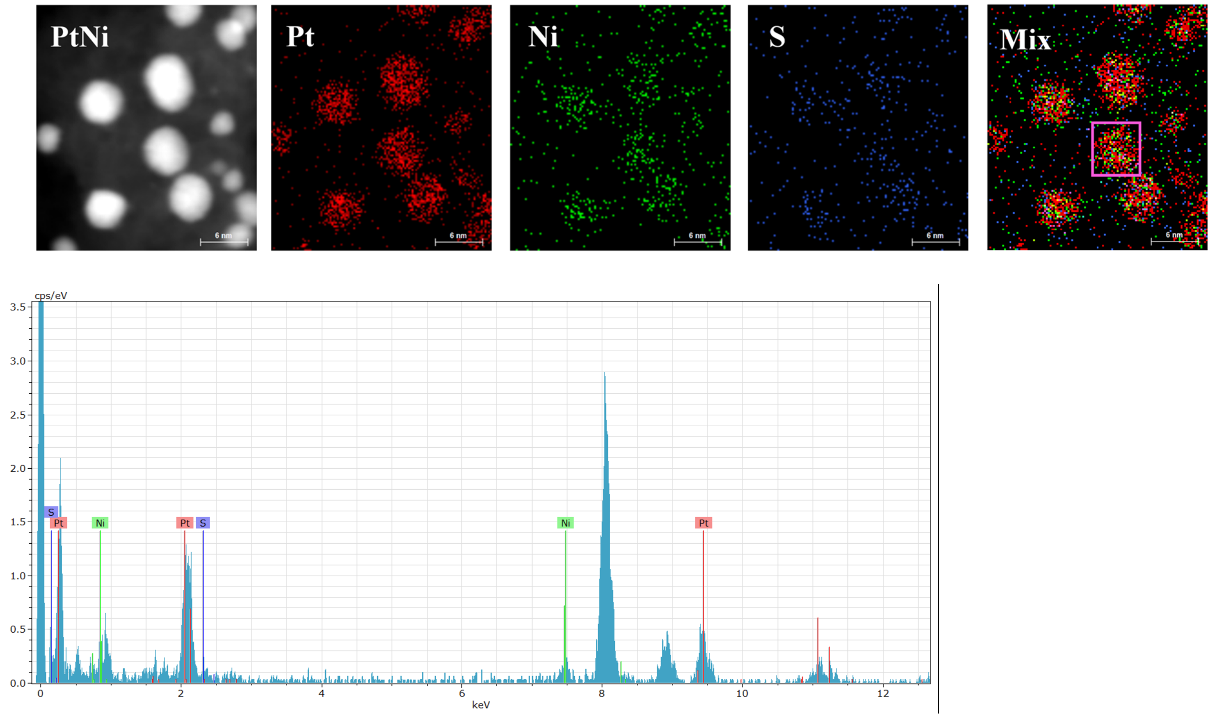


**Supplementary Figure 6.** EDS elemental mapping and EDS spectra of the PtNi IMCs catalyst.

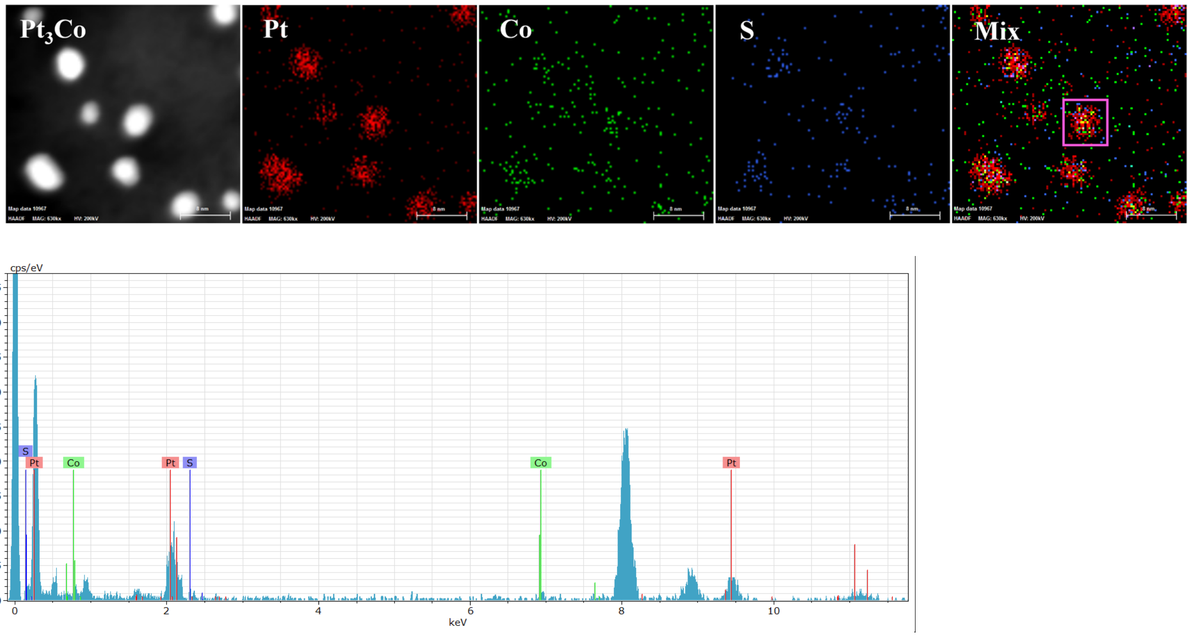


**Supplementary Figure 7.** EDS elemental mapping and EDS spectra of the $Pt_3Co$ IMCs catalyst.

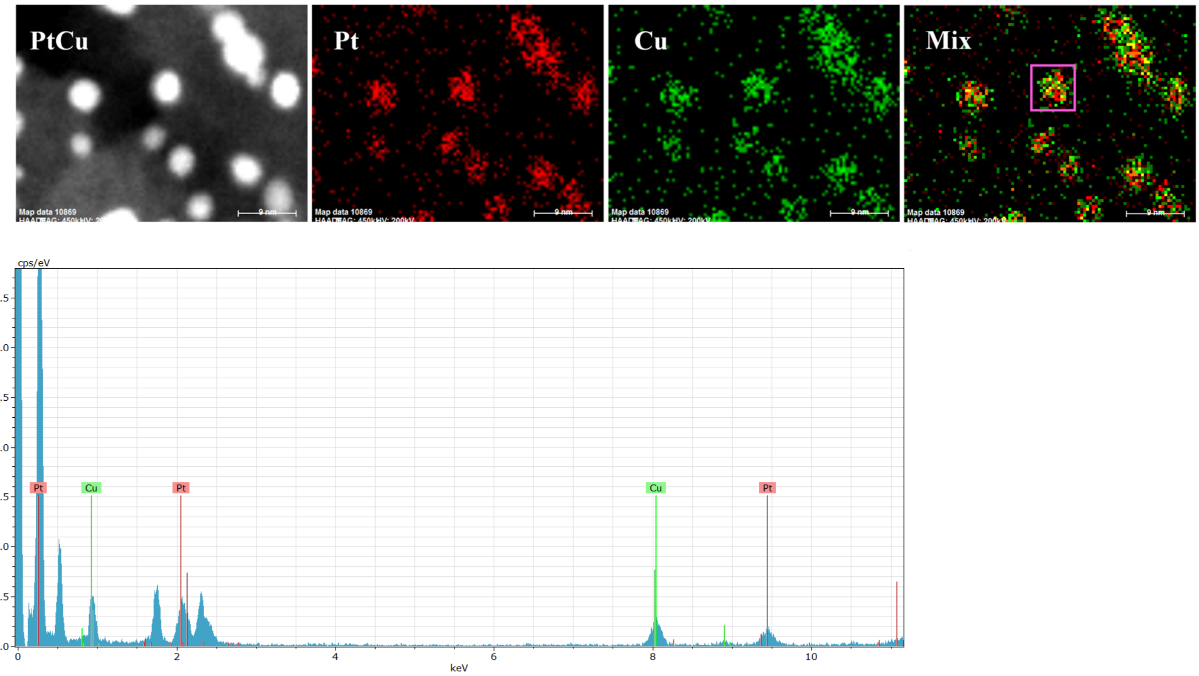


**Supplementary Figure 8.** EDS elemental mapping and EDS spectra of the PtCu IMCs catalyst. Molybdenum microgrid was used instead of cooper microgrid for the EDS measurements.

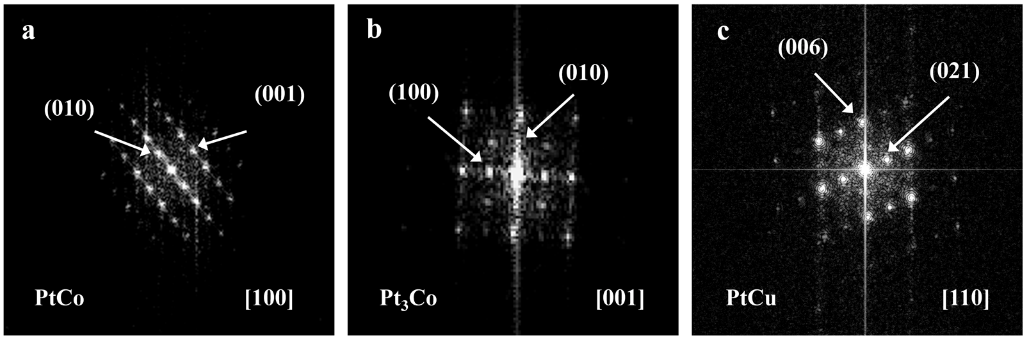


**Supplementary Figure 9.** FFT patterns of PtCo (a), $Pt_3Co$ (b), and PtCu (c) catalysts whose atomic-resolution HAADF-STEM images were shown in Fig 4.

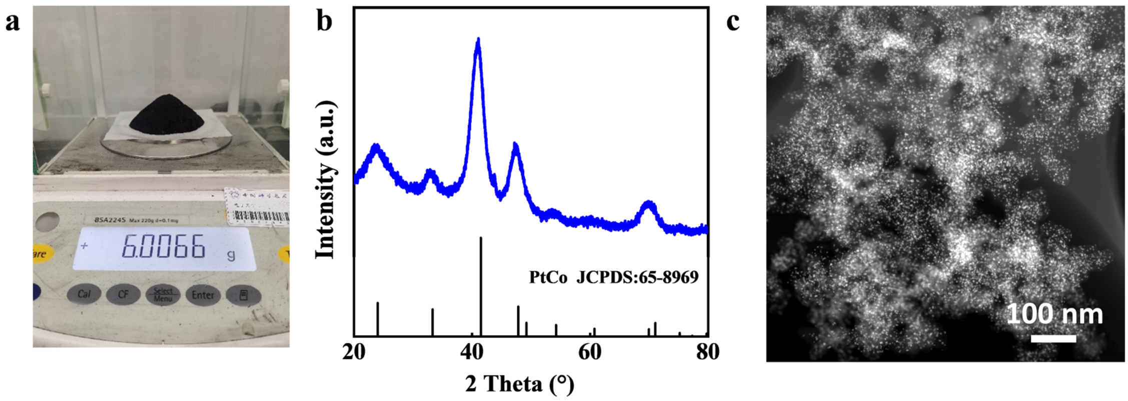


**Supplementary Figure 10.** (a) Photograph showing the large-scale synthesis of the PtCo IMCs catalyst with STG as additives, the one-batch production could exceeded 6 grams. (b) XRD patterns and (c) HAADF-STEM image of the PtCo IMCs catalyst synthesized in grams scale.

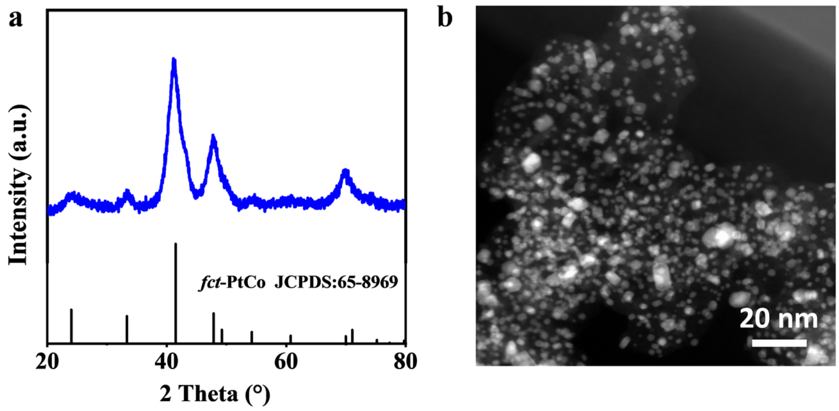


**Supplementary Figure 11.** (a) XRD patterns and (b) HAADF-STEM image of 45 wt% PtCo prepared with STG additives.

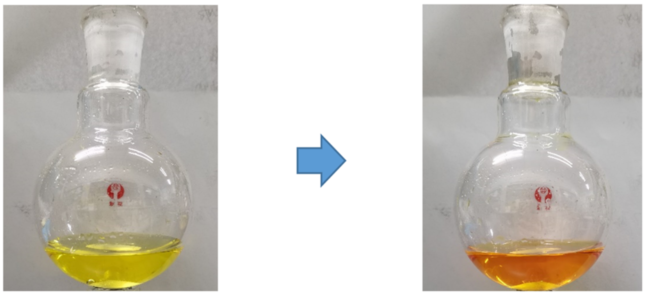

$H_2PtCl_6 \cdot 6H_2O$ (aq) $H_2PtCl_6 \cdot 6H_2O$ (aq) + STG

**Supplementary Figure 12.** Photographs showing the discoloration of $H_2PtCl_6 \cdot 6H_2O$ solution when adding STG.

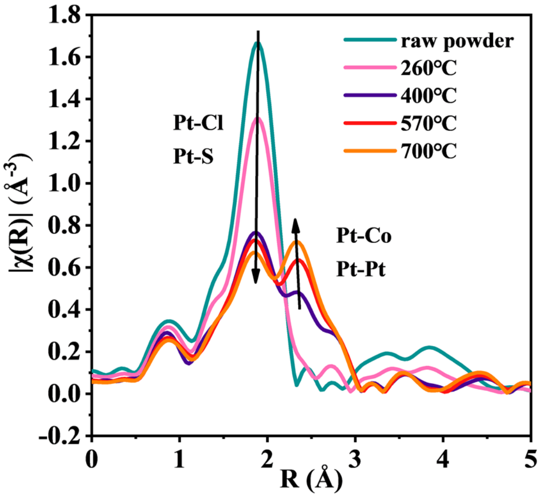


**Supplementary Figure 13.** R space of the XAFS results for the samples obtained after annealing of STG-$H_2PtCl_6$-$CoCl_2$/C precursor at different temperatures for 10 min.

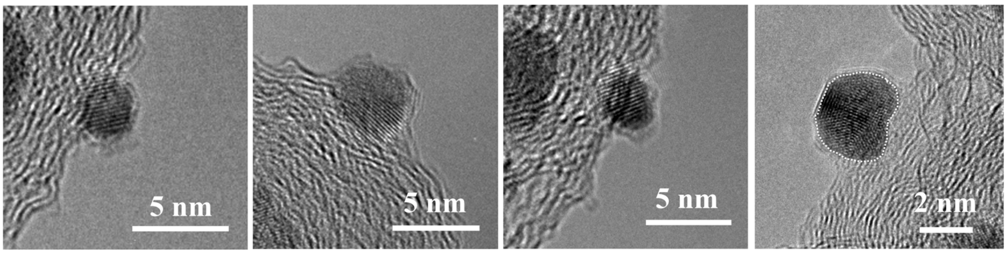


**Supplementary Figure 14.** High-resolution bright-field STEM images of the PtCo IMCs catalyst prepared with STG additives, showing the formation of thin carbon coating around PtCo particle.

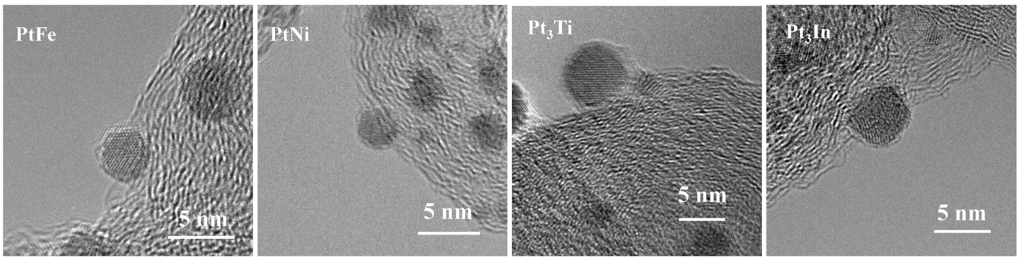


**Supplementary Figure 15.** High-resolution bright-field STEM images of PtFe, PtNi, $Pt_3Ti$, and $Pt_3In$ IMCs catalyst prepared with STG additives.

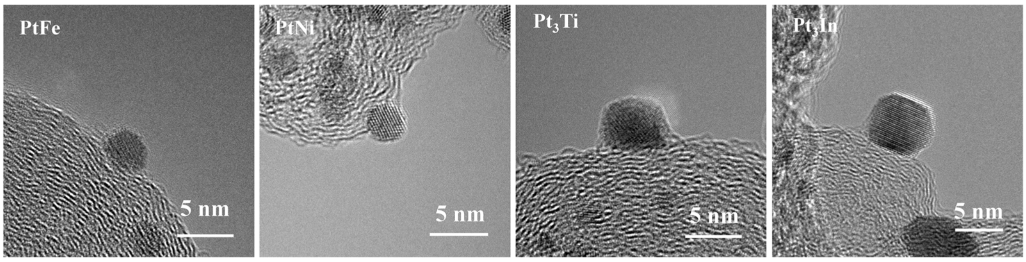


**Supplementary Figure 16.** High-resolution bright-field STEM images of STG-assisted PtFe, PtNi, $Pt_3Ti$, and $Pt_3In$ IMCs catalyst after air oxidation.

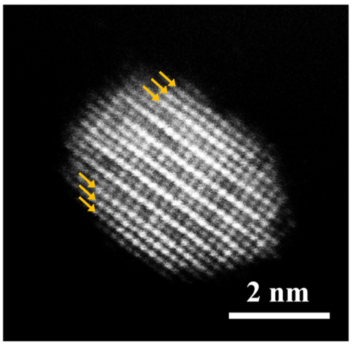


**Supplementary Figure 17.** Atomic-resolution HAADF-STEM image of the post-treated PtCo IMCs catalyst that was composed of an intermetallic PtCo core and two to three atomic layers of Pt shell.

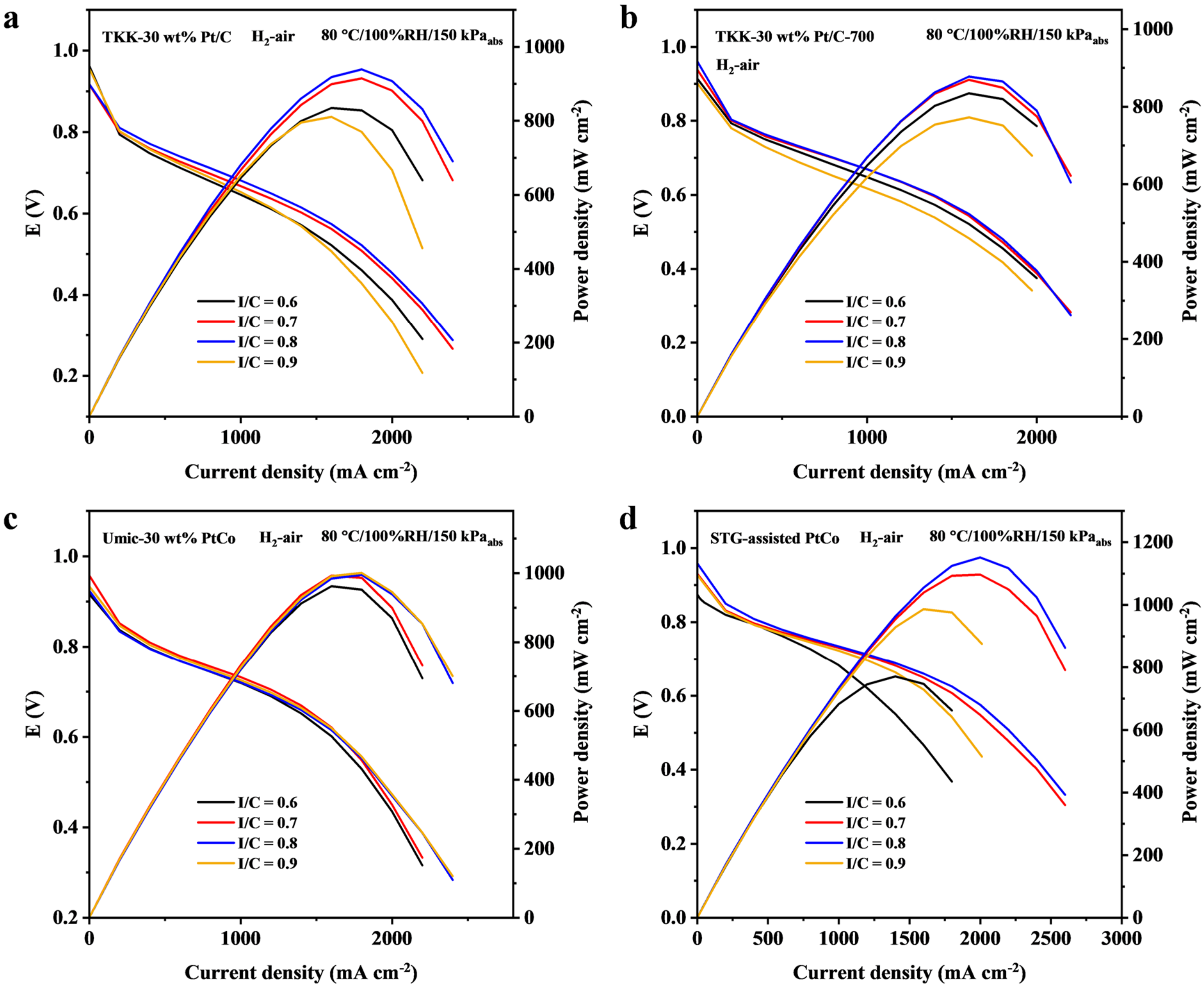


**Supplementary Figure 18.** The I/C ratio optimization process of TKK-30 wt% Pt/C (a), TKK-30 wt% Pt/C-700 (b), Umic-30 wt% PtCo (c), and STG-assisted PtCo (d) catalysts. The I/C ratio ranged from 0.6 to 0.9, and the MEAs made with catalysts of TKK-30 wt% Pt/C, TKK-30 wt% Pt/C-700, and STG-assisted PtCo exhibited the optimal performance with the I/C ratio of 0.8, while the Umic-30 wt% PtCo exhibited the optimal performance when the I/C is 0.9.

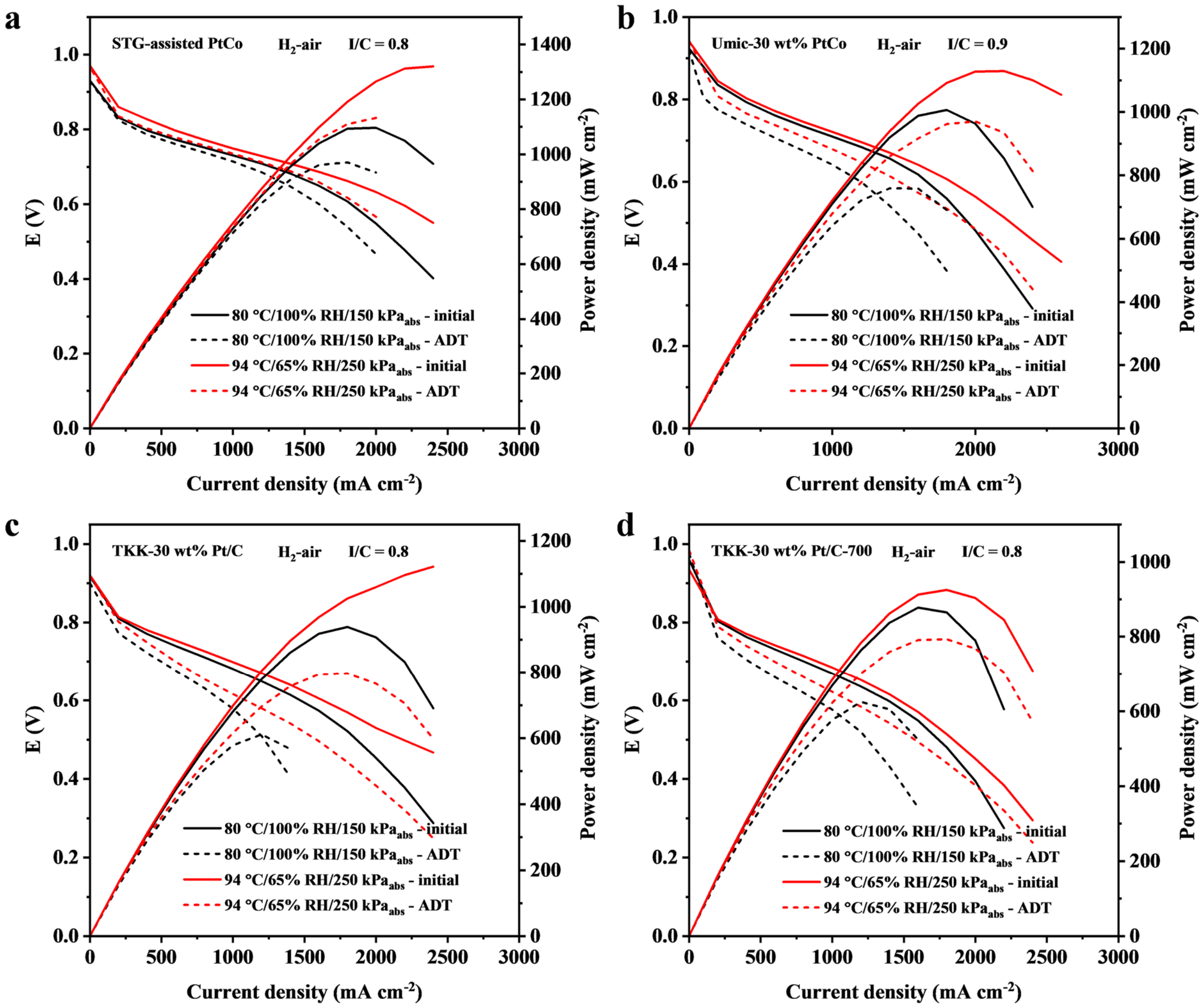


**Supplementary Figure 19.** $H_2$-air polarization curves and power density plots of STG-assisted PtCo (a), Umic-30 wt% PtCo (b), TKK-30 wt% Pt/C (c), and TKK-30 wt% Pt/C-700 (d) at the beginning and after 30,000 cycles' ADT in the single-cell tests. All the catalysts used the optimal I/C ratio. Test conditions: 80 °C, 100% RH, 150 kPa$_{abs}$, or 94 °C, 65% RH, 250 kPa$_{abs}$.

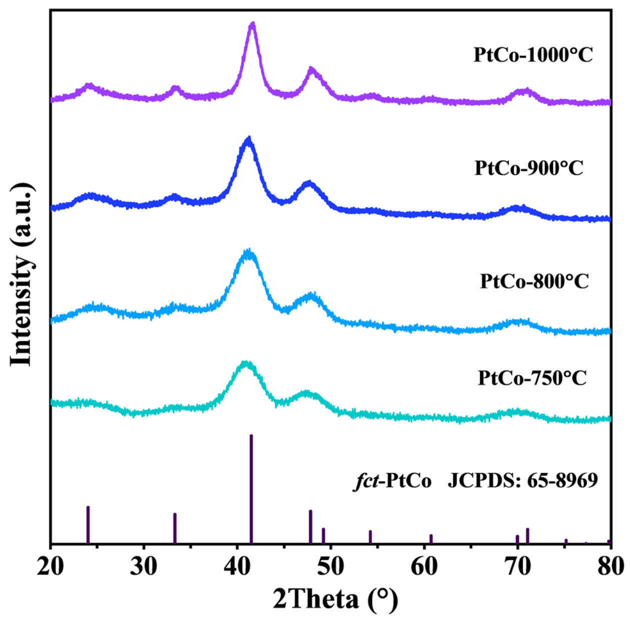


**Supplementary Figure 20.** XRD patterns of the PtCo catalysts prepared with STG additive at different temperatures, showing the gradually increased average particle size and ordering degree with temperature.

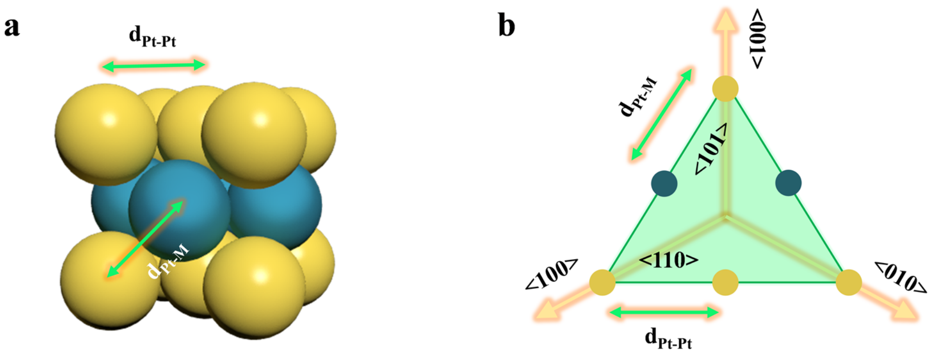


**Supplementary Figure 21.** (a) Crystal structure of *fct*-PtM, yellow balls represent Pt, blue balls correspond M (M is Mn, Fe, Co, Ni, or Zn). (b) Schematic illustration of lattice mismatch of (111) facet, yellow circles represent Pt and blue circles represent M.

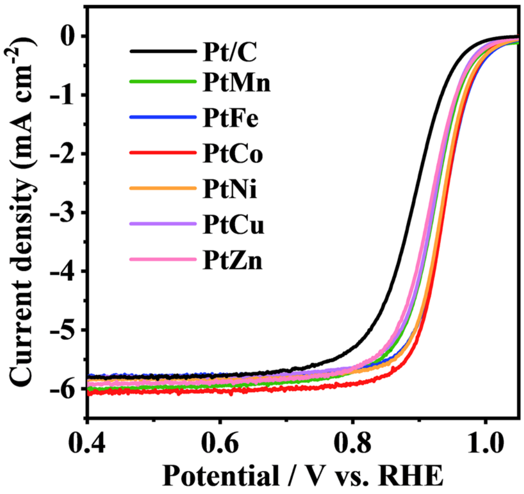


**Supplementary Figure 22.** RDE polarization curves of the five $L1_0$ PtM IMCs, the $L1_1$ PtCu IMCs, and the commercial TKK-30 wt% Pt/C.

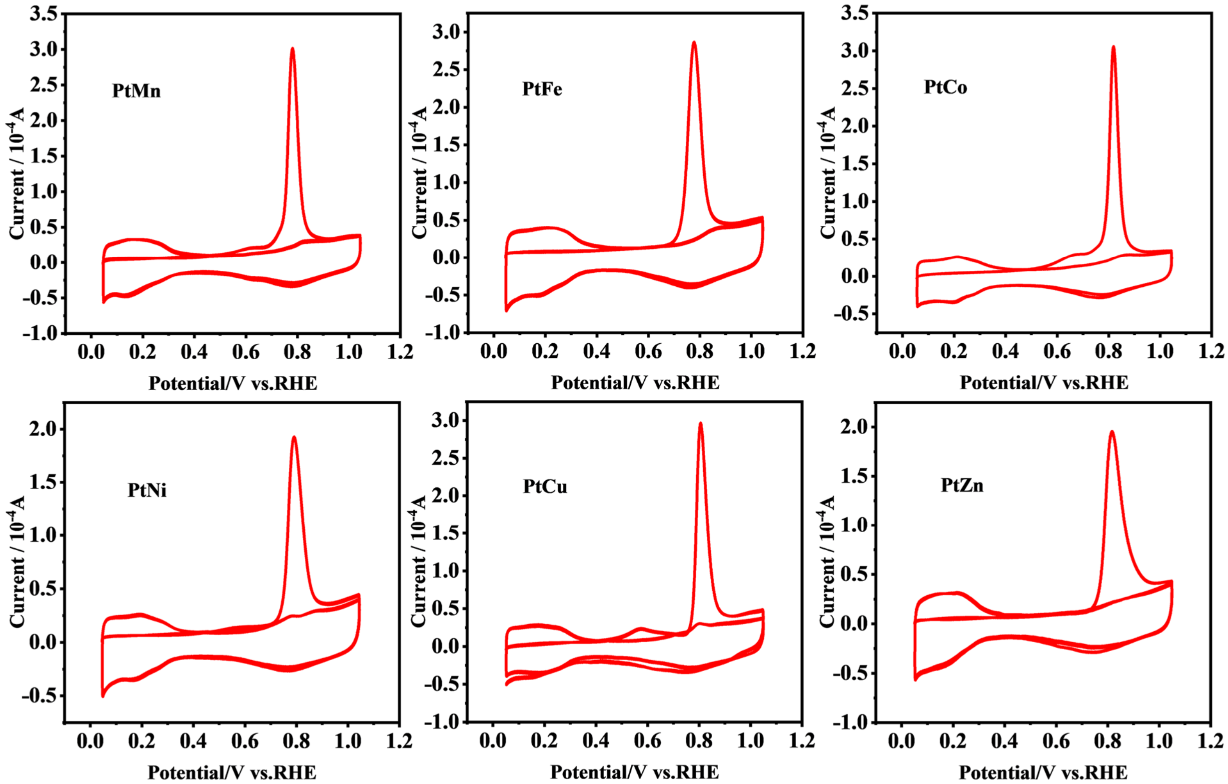


**Supplementary Figure 23.** CO-stripping curves of the IMCs catalysts for the ECSA measurements. The corresponding values of ECSA were listed in Supplementary Table 6.

**Supplementary Table 1.** Average particle sizes of the PtCo samples prepared with different molecule additives at 700 °C.

| Sample | XRD size (nm) | STEM size (nm) |
|---|---|---|
| PtCo-Additive free | 14.9 | 12.9 |
| PtCo-BZF | 12.4 | 9.5 |
| PtCo-GLU | 9.6 | 8.8 |
| PtCo-SAc | 8.3 | 7.7 |
| PtCo-APR | 6.4 | 5.7 |
| PtCo-SGC | 4.8 | 5.5 |
| PtCo-DCDA | 5.5 | 5.4 |
| PtCo-MUA | 4.3 | 3.4 |
| PtCo-MBM | 3.5 | 3.0 |
| PtCo-MPA | 2.4 | 2.3 |
| PtCo-STG | 2.8 | 2.5 |

**Supplementary Table 2.** Average particle sizes of the 18 Pt-IMCs catalysts prepared with and without STG additive from XRD results. The optimal annealing procedure and ordering degree of the Pt-IMCs prepared with STG additive were also listed.

| Sample | XRD size (nm) | | Optimal annealing procedure | Ordering degree (%) |
|---|---|---|---|---|
| | With STG | STG-free | | |
| $Pt_3Al$ | 4.9 | 9.7 | 900/2h | 27[a] |
| $Pt_3Ti$ | 4.3 | 8.8 | 900/2h-600/6h | 35[a] |
| $Pt_3V$ | 5.4 | 10.4 | 1000/2h-600/6h | 35[a] |
| $Pt_3Cr$ | 4.3 | 8.7 | 900/2h-600/6h | 82[a] |
| $Pt_3Mn$ | 4.1 | 8.3 | 800/2h-600/6h | 75[a] |
| PtMn | 4.5 | 10.0 | 900/2h-600/6h | 49[b] |
| $Pt_3Fe$ | 4.8 | 8.5 | 900/2h-600/6h | 73[a] |
| PtFe | 3.5 | 8.9 | 900/2h-700/6h | 76[c] |
| $Pt_3Co$ | 5.2 | 8.2 | 900/2h-600/6h | 82[a] |
| PtCo | 3.3 | 9.2 | 900/2h-600/6h | 72[c] |
| PtNi | 3.4 | 8.6 | 900/2h-550/6h | 53[c] |
| PtCu | 3.0 | 8.7 | 800/2h-600/6h | — |
| $PtCu_3$ | 3.5 | 12.2 | 900/2h-600/6h | 34[d] |
| PtZn | 4.7 | 9.5 | 900/2h-600/6h | 51[b] |
| $Pt_3Ga$ | 5.4 | 11.1 | 900/2h | 77[a] |
| $Pt_3Ge$ | 5.6 | 11.3 | 900/2h | — |
| $Pt_3In$ | 4.2 | 11.5 | 900/2h | 96[a] |
| $Pt_3Sn$ | 4.7 | 8.3 | 900/2h | 94[a] |

[a] $S_{(110)}/S_{(111)}$

[b] $S_{(110)}/[S_{(111)}+S_{(200)}]$

[c] $S_{(110)}/[S_{(111)}+S_{(200)}+S_{(002)}]$

[d] $I_{(110)}/I_{(111)}$

**Supplementary Table 3.** Type and dosage of Pt and non-Pt precursors used for the synthesis of Pt-IMCs libraries.

| Sample | Pt precursor | | Non-Pt precursor | |
|---|---|---|---|---|
| | Type | Dosage (mmol) | Type | Dosage (mmol) |
| $Pt_3Al$ | | 0.13 | $AlCl_3 \cdot 6H_2O$ | 0.052 |
| $Pt_3Ti$ | | 0.203 | $TiCl_4$ | 0.068 |
| $Pt_3V$ | | 0.202 | $VCl_3$ | 0.067 |
| $Pt_3Cr$ | | 0.202 | $CrCl_3 \cdot 6H_2O$ | 0.067 |
| $Pt_3Mn$ | | 0.131 | $MnCl_2 \cdot 4H_2O$ | 0.052 |
| PtMn | | 0.171 | $MnCl_2 \cdot 4H_2O$ | 0.206 |
| $Pt_3Fe$ | | 0.2 | $FeCl_3$ | 0.067 |
| PtFe | | 0.171 | $FeCl_3$ | 0.205 |
| $Pt_3Co$ | $H_2PtCl_6 \cdot 6H_2O$ | 0.2 | $CoCl_2 \cdot 6H_2O$ | 0.067 |
| PtCo | | 0.168 | $CoCl_2 \cdot 6H_2O$ | 0.252 |
| PtNi | | 0.169 | $NiCl_2 \cdot 6H_2O$ | 0.203 |
| PtCu | | 0.166 | $Cu(NO_3)_2 \cdot 3H_2O$ | 0.182 |
| $PtCu_3$ | | 0.111 | $Cu(NO_3)_2 \cdot 3H_2O$ | 0.4 |
| PtZn | | 0.165 | $Zn(NO_3)_2 \cdot 6H_2O$ | 0.197 |
| $Pt_3Ga$ | | 0.132 | $GaCl_3$ | 0.053 |
| $Pt_3Ge$ | | 0.132 | $GeCl_4$ | 0.053 |
| $Pt_3In$ | | 0.135 | $InCl_3$ | 0.054 |
| $Pt_3Sn$ | | 0.135 | $SnCl_2 \cdot 2H_2O$ | 0.054 |

**Supplementary Table 4.** The atomic ratio results obtained by EDS mapping of Supplementary Figures 4-8.

| Sample | Atomic ratio (%) | | |
| --- | --- | --- | --- |
| | Pt | M | S |
| PtFe | 47.4 | 42.5 | 10.1 |
| PtCo | 47.5 | 45.2 | 7.3 |
| PtNi | 47.2 | 44.1 | 8.7 |
| $Pt_3Co$ | 71.8 | 23.7 | 4.5 |
| PtCu | 54.8 | 45.2 | -- |

**Supplementary Table 5.** Average particle sizes from XRD and the ordering degree of additional PtCo IMCs catalysts prepared with STG additives, including the ones prepared at different temperatures, the one synthesized in grams scale, and the one with a high metal loading of 45 wt%.

| Sample | XRD size (nm) | Ordering degree (%) |
|---|---|---|
| PtCo-750ºC | 2.3 | 53 |
| PtCo-800ºC | 2.5 | 63 |
| PtCo-900ºC | 3.6 | 72 |
| PtCo-1000ºC | 4.5 | 79 |
| Large-scale PtCo | 4.3 | 65 |
| 45 wt% PtCo | 4.7 | 56 |

**Supplementary Table 6.** ECSA, mass activity, and specific activity of the commercial TKK-30 wt% Pt/C and the STG-assisted PtM IMCs catalysts. The mass activity and specific activity were obtained at 0.9 V vs RHE, and the electrochemical tests were measured in thin film-RDE (10 µg catalyst on 0.196 $cm^2$ disk).

| Sample | ECSA ($m^2\ g_{Pt}^{-1}$) | Mass activity ($A\ mg_{Pt}^{-1}$) | Specific activity ($mA\ cm^{-2}$) |
|---|---|---|---|
| Pt/C | 72.5 | 0.35 | 0.48 |
| PtMn | 75.1 | 1.12 | 1.49 |
| PtFe | 86.7 | 2.18 | 2.51 |
| PtCo | 70.1 | 2.25 | 3.21 |
| PtNi | 63.4 | 2.11 | 3.33 |
| PtCu | 74.8 | 1.18 | 1.57 |
| PtZn | 78.8 | 0.88 | 1.12 |

**Supplementary Table 7.** Calculated surface strain of the five $L1_0$ PtM IMCs catalysts. Negative values indicate compression strain.

| Sample | Surface strain (%) |
|---|---|
| PtMn | -1.83% |
| PtFe | -3.84% |
| PtCo | -8.24% |
| PtNi | -8.97% |
| PtZn | -2.74% |

**Supplementary Table 8.** A detailed comparison of MEA performance of STG-assisted PtCo, Umic-30 wt% PtCo, TKK-30 wt% Pt/C, and TKK-30 wt% Pt/C-700 in $H_2$-air single-cell test.

| Sample | Current density ($mA\ cm^{-2}$) 80 °C/100%RH/150 $kPa_{abs}$ | | Power density ($W\ cm^{-2}$) 80 °C/100%RH/150 $kPa_{abs}$ | | Mass activity at 0.9 V ($A\ mg_{Pt}^{-1}$) | | | Voltage loss at 0.8 A $cm^{-2}$ (mV) | | Rated power density ($W\ cm^{-2}$) 94 °C/65%RH/250 $kPa_{abs}$ | |
|---|---|---|---|---|---|---|---|---|---|---|---|
| | at 0.8 V | at 0.6 V | at 0.8 V | at 0.6 V | initial | After ADT | DOE 2025 target | | | initial | ADT |
| TKK-30 wt% Pt/C | 250 | 1470 | 0.20 | 0.88 | 0.32 | 0.15 | ≥ 0.44 A $mg_{Pt}^{-1}$<br>≤ 40% loss after ADT | 83 | DOE 2025 target: ≤ 30 mV loss after ADT | 0.79 | 0.49 |
| TKK-30 wt% Pt/C -700 | 216 | 1390 | 0.17 | 0.83 | 0.28 | 0.19 | | 81 | | 0.73 | 0.51 |
| Umic-30 wt% PtCo | 395 | 1659 | 0.32 | 0.99 | 0.86 | 0.58 | | 76 | | 0.94 | 0.71 |
| STG-assisted PtCo | 412 | 1821 | 0.33 | 1.09 | 1.08 | 0.81 | | 21 | | 1.17 | 1.03 |